

A unified multiaxial fatigue damage model for isotropic and anisotropic materials

Yongming Liu, Sankaran Mahadevan *

Vanderbilt University, Nashville, TN 37235, USA

Received 21 May 2005; received in revised form 15 January 2006; accepted 2 March 2006

Available online 11 May 2006

Abstract

A unified multiaxial fatigue damage model based on a characteristic plane approach is proposed in this paper, integrating both isotropic and anisotropic materials into one framework. Compared with most available critical plane-based models for multiaxial fatigue problem, the physical basis of the characteristic plane does not rely on the observations of the fatigue crack in the proposed model. The cracking information is not required for multiaxial fatigue analysis and the proposed model can automatically adapt for very different materials experiencing different failure modes. The effect of the mean normal stress is also included in the proposed model. The results of the proposed fatigue life prediction model are validated using experimental results of metals as well as unidirectional and multidirectional composite laminates.

© 2006 Elsevier Ltd. All rights reserved.

Keywords: Multiaxial fatigue; Characteristic plane; Metals; Composite laminates

1. Introduction

Many critical mechanical components experience multiaxial cyclic loading during their service life. In recent decades, numerous attempts to develop multiaxial fatigue damage modeling have been reported. The multiaxial fatigue problem of engineering materials is mainly caused by two reasons. In isotropic materials, the multiaxial stress within the material is due to the complex applied loading history. In anisotropic materials, a multiaxial stress state is obtained even if the applied loading is uniaxial. Different from the uniaxial fatigue problem, the multiaxial fatigue problem is more complex due to the complex stress states, loading histories and possible anisotropy of the material.

For isotropic materials, mainly metals, several reviews and comparisons of existing multiaxial fatigue models can be found [17,3,67,51,45,65]. Fatigue damage models

can be based on one of several criteria: stress, strain, energy or damage mechanics. This paper focused on stress-based approaches for multiaxial high-cycle fatigue, which can be divided into four groups: equivalent stress approach [37,1,21], stress invariant approach [57,8,28], average stress approach [51], and critical plane stress approach [47,15,48,5,52]. Although there are many proposed models for multiaxial fatigue damage modeling, most of them are limited to specific materials or loading conditions [51]. The authors [41] proposed a new stress-based characteristic plane model for metals, which performs well for both brittle and ductile metals. The characteristic plane approach has been extended for low-cycle multiaxial fatigue problem using $e-N$ curves [43].

The above discussion is for isotropic materials. However, many engineering materials exhibit some degree of anisotropy in mechanical properties, such as rolled metals. Moreover, strongly anisotropic materials such as composite laminates are being used in the industry more popularly in the recent decades. Unlike the extensive progress in multiaxial fatigue analysis of isotropic materials, much further

* Corresponding author. Tel.: +1 615 322 3040; fax: +1 615 322 3365.
E-mail address: Sankaran.Mahadevan@vanderbilt.edu (S. Mahadevan).

effort is needed to include the anisotropy of the material [16,40,56,12]. Several investigations have been reported for anisotropic composite laminates. Degrieck and Van Paepegem [11] classify existing fatigue models into three categories: fatigue life model (S–N curves), residual strength or residual stiffness model, and progressive damage model. Hasin and Rotem [22] proposed a failure criterion which mimic the form of static strength criterion, based on two major failure modes (fiber failure and matrix failure). Reifsnider and Gao [55] proposed a micromechanics based model which can take into account the interfacial bond. Wu, Jen and Lee [66,24] proposed different failure criteria based on the Tsai-Hill criterion. Philippidis and Vassilopoulos [54] proposed a failure criterion based on the Tsai-Wu criterion. Petermann and Plumtree [53] proposed a critical plane model for unidirectional laminates under off-axis tension–tension fatigue loading. Kawai, Kawai et al., [32,31] proposed an effective stress model for the unidirectional laminates under off-axis loading, which is based on the Tsai-Hill static strength theory. Liu and Mahadevan [42] proposed a damage accumulation model for multidirectional laminates under tension–tension fatigue loading. Most of the fatigue models for anisotropic composite laminates are for single applied off-axis loading, which causes proportional multiaxial stress state within the laminates. Very few theoretical and experimental studies are found in the literature for the non-proportional multiaxial fatigue analysis of general anisotropic materials.

To the authors' knowledge, no single existing multiaxial fatigue damage model is universally accepted for different materials (i.e. metals and composites) and different loading conditions (i.e. proportional and non-proportional multiaxial loading). In this paper, a unified multiaxial fatigue damage model is proposed for both isotropic and anisotropic materials.

In this paper, a new fatigue damage model named characteristic plane-based model is proposed as a unified approach for both isotropic and anisotropic materials. The characteristic plane approach is similar with the critical plane in the calculation procedure. A plane is first determined and the stress components on the plane are combined together and used for fatigue life prediction. Unlike most of existing critical plane-based models, the characteristic plane in the proposed model is not based on the physical observations of the crack but arises from the idea of dimension reduction. It assumes the complex multiaxial fatigue problem can be approximated by using the stress components on a certain plane (named characteristic plane in this paper). Then the objectives are to find the plane and the formula of combinations of the stress components on that plane. Through this type of definition of the characteristic plane, failure mode analysis is not required and the proposed model can automatically adapt for different materials. The correction factor for the mean normal stress is also introduced to the proposed model. A wide range of experimental observations for metals and composite laminates available in the literature are used

to validate the proposed model. Very good correlations are found between predicted and experimental fatigue lives under proportional and non-proportional loading for very different materials.

2. Multiaxial fatigue model for isotropic material

The characteristic plane is a material plane on which the fatigue damage is evaluated. In the proposed method, the complex stress time history functions are used to calculate an "equivalent" stress on the characteristic plane. The equivalent stress is used to correlate with the fatigue damage. Most of the available models based on the critical plane approach assume that the critical plane is fixed. The critical plane is assumed to coincide with either the maximum normal strain/stress plane (Mode I) or the maximum normal strain/stress plane (Mode II). The applicability of the fatigue model becomes limited if the critical plane is fixed [41,43].

The failure types of metals can be classified as shear dominated, tensile dominated and mixed under multiaxial loading. They are related to the microcrack nucleation and propagation along the persistent slip bands, along grain boundaries, across the grain, void cleavage, etc. The failure types of composite laminates are much more complex and fundamentally different with those of metals, such as matrix cracking, fiber breakage, fiber–matrix interfacial fracture, delamination, etc. Any attempt to build a failure mechanism-based model for both isotropic metals and anisotropic composites would be rather difficult or impossible, as they are very different materials and have unique failure types.

Liu and Mahadevan [41,43] have proposed a characteristic plane approach for multiaxial fatigue analysis of metals, which does not rely on the failure mechanisms of materials and only depends on the quantitative S–N (e–N) curves under uniaxial and pure torsional fatigue loading. It has been shown that the model performs well under different failure mechanisms of metals. Even without knowing the failure mechanism, the proposed method can still be applied [43].

The stress version of the characteristic plane approach [41] is used in this paper. The detailed derivation of the multiaxial fatigue model can be found in the previous publication by the same authors [41]. Only a brief summary and results are presented here.

2.1. Multiaxial fatigue model

A new fatigue damage criterion [41] was proposed based on the non-linear combination of the normal stress amplitude, shear stress amplitude and hydrostatic stress amplitude acting on the characteristic plane, as

$$\sqrt{\left(\frac{\sigma_{a,z}}{f_{-1}}\right)^2 + \left(\frac{\tau_{a,z}}{t_{-1}}\right)^2 + k\left(\frac{\sigma_{a,z}^H}{f_{-1}}\right)^2} = \beta \quad (1)$$

where $\sigma_{a,\alpha}$, $t_{a,\alpha}$ and $\sigma_{a,\alpha}^H$ are the normal stress amplitude, shear stress amplitude and hydrostatic stress amplitude acting on the characteristic plane, respectively; α is the angle between the characteristic plane and the maximum normal stress plane; f_{-1} and t_{-1} are fatigue limits in fully reversed uniaxial and torsional tests, respectively; and k and β are material parameters which can be determined by uniaxial and torsional fatigue limits. The coefficient k has a physical meaning: it is the contribution of the hydrostatic stress amplitude to the multiaxial fatigue damage. Since the fatigue damage process is a monotonically increasing process, k has to be non-negative.

The characteristic plane-based approach for multiaxial fatigue problem is a dimensional reduction from a mathematic point of view. It tries to approximate the complex 3D stress (strain) fatigue damage process only using the stress (strain) components on a certain plane. This approximation arises from a basic question. Does the out-of-plane stress (strain) contribute to the multiaxial fatigue damage? Suppose the same material is under two different multiaxial stress states, which result in the same stress amplitude on the characteristic plane but different stress amplitude out of the plane. Will the material experience the same fatigue life or not? Both in-plane and out-of-plane stress effects are considered in the proposed method, but they are treated differently. To consider the out-of-plane stress components, two possible ways can be used. One is to use the out-of-plane stress directly. The other is to use the hydrostatic stress amplitude as it contains the out-of-plane stress components. We choose the hydrostatic stress amplitude as the mechanical parameter in the proposed model based on the following reasons: (1) it is easy to extend to general 3D stress state. If a general 3D stress state is considered (i.e. two out-of-plane stresses exist and need to be considered), the method using the out-of-plane stress components need to add a term in the criteria, which makes the model more complex compared with the method using the hydrostatic stress amplitude. Also, the hydrostatic stress amplitude is easy to calculate under some situations. For example, for far field non-proportional bending-torsional fatigue problem, the hydrostatic stress amplitude can be calculated directly as it is the first invariant of the stress tensor. The out-of-plane stress components must be calculated by stress transformation and searching. (2) The comparison with various experimental data [41,43] shows the proposed method (using the hydrostatic stress amplitude) has a good agreement with experimental observations. So we decide to use the hydrostatic stress amplitude rather than to use the out-of-plane stress amplitude directly.

Two special orientations of the characteristic plane using the proposed fatigue damage parameter (Eq. (1)) have been discussed in Liu and Mahadevan [41]. One type assumes that the characteristic plane is the maximum normal stress (or strain) plane (Mode I), which is same with some critical plane-based models [60,62,7,34]. The other assumes that the critical plane coincides with the maximum shear stress (or strain) plane (Mode II), which is same with

some critical plane-based models [4,27,44,61,14,19,13,50]. Based on the analysis using these two different characteristic plane orientations, several conclusions can be drawn [41]. The contribution of the hydrostatic stress amplitude is different for different materials if the characteristic plane orientation is fixed. Neither of the two characteristic plane orientation assumptions can be applied to the whole range of materials (i.e. from brittle to ductile materials). For the two special types of material ($t_{-1}/f_{-1} = 1$ and $t_{-1}/f_{-1} = 1/\sqrt{3}$), the contribution of the hydrostatic stress amplitude is zero if the characteristic plane is defined as the maximum normal stress amplitude plane or the maximum shear stress amplitude plane, respectively.

So instead of fixing the characteristic plane, the current model searches for the characteristic plane orientations on which the contribution of the hydrostatic stress amplitude is minimized to zero. By using this approach, the applicability of the proposed method is extended to both brittle and ductile materials. This strategy leads to the analytical solutions for the material parameters summarized in Table 1 [41].

In Table 1, $s = \frac{t_{-1}}{f_{-1}}$ is the fatigue strength ratio under the torsional loading and the uniaxial loading. Materials with $t_{-1}/f_{-1} \leq 1/\sqrt{3}$ are usually known as ductile (mild) metals, whereas materials with $1/\sqrt{3} \leq t_{-1}/f_{-1} \leq 1$ are usually known as brittle (hard) metals [5]. Materials with $t_{-1}/f_{-1} \geq 1$ are referred as extremely brittle (hard) metals by Liu and Mahadevan [41]. Thus, the model is found to be applicable to both brittle and ductile materials. As shown in Table 1, The characteristic plane coincides with usually defined crack growth planes (Mode I and Mode II) under two conditions. For the material with $t_{-1}/f_{-1} \geq 1$, the characteristic plane is the maximum normal stress amplitude plane (Mode I). For the material with $t_{-1}/f_{-1} = 1/\sqrt{3}$, the characteristic plane is the maximum shear stress amplitude plane (Mode II).

The implementation is quite simple. For any arbitrary multiaxial loading history, the maximum stress amplitude plane is identified first. This is achieved by enumeration, by changing the angle by 1° increment. Then the angle α and material parameters are determined for different materials according to Table 1. The angle between the characteristic plane and the maximum normal stress amplitude plane is α . Finally, the stress components on the characteristic plane are calculated and the fatigue damage is evaluated using Eq. (1). Note that the characteristic plane in the proposed model depends not only on the stress state (maximum normal stress amplitude plane) but also on the material property (angle α).

Table 1
Material parameters for fatigue damage evaluation

Material property	$s = \frac{t_{-1}}{f_{-1}} \leq 1$	$s = \frac{t_{-1}}{f_{-1}} > 1$
α	$\cos(2\alpha) = \frac{-2 + \sqrt{4 - 4(1/s^2 - 3)(5 - 1/s^2 - 4s^2)}}{2(5 - 1/s^2 - 4s^2)}$	$\alpha = 0$
k	$k = 0$	$k = 9(s^2 - 1)$
β	$\beta = [\cos^2(2\alpha)s^2 + \sin^2(2\alpha)]^{\frac{1}{2}}$	$\beta = s$

2.2. Mean stress effect

Practical mechanical components generally experience cyclic fatigue loading together with the mean stress. The mean stress could also be introduced by residual stress, environmental effects, etc. It is well known that the mean normal stress has an important effect on fatigue life. Normally, tensile mean stress reduces the fatigue life, while compressive mean stress increases the fatigue life [58].

There are many models for mean normal stress effect correction. Gerber, Goodman, Soderberg and Morrow [18,20,64,49] proposed different correction factors. Kujawski and Ellyin [35] proposed a unified approach to mean stress effect. For the multiaxial fatigue problem, mean normal stress is included in the model in different ways [63] depending on different models. Fatemi and Socie [14] considered the maximum normal stress acting on the critical plane. Papadopoulos [51] considered the hydrostatic mean stress. Farahani [13] used a correction factor based on the mean stress on the critical plane.

The mean shear stress effect is very complex especially for the multiaxial fatigue problem and needs further study. There is still much argument as to the proper way to include this effect. Sines [57] stated that a superimposed mean static torsion has no effect on the fatigue limit of metals subjected to cyclic torsion. A similar conclusion was also found by Davoli et al. [10]. The mean shear stress effect is often neglected in the high cycle fatigue analysis for metals [10]. The mean shear stress effect can not be neglected for finite fatigue life prediction. It is known that the mean shear stress effect for metals increases as the fatigue life decreases. For composite materials, very few studies can be found in the open literature about the mean shear stress effect on the multiaxial fatigue life. In the current study, we only collect data with no mean stress and with mean normal stress for model validation. The main objective of the current study is to propose a general multiaxial model for different materials (i.e. metals and composites). A detailed study about the mean shear stress effect is beyond the scope of the current study and needs to be explored in the future. Therefore in the current model, the mean shear stress effect is not considered.

Based on the experimental data collected from the literature, the mean normal stress is introduced into the fatigue model in this paper by a correction factor $(1 - \frac{\sigma_{m,max}}{f_{ref}})$. Thus, Eq. (1) is rewritten as:

$$\frac{1}{\left(1 - \frac{\sigma_{m,max}}{f_{ref}}\right)} \sqrt{\left(\frac{\sigma_{a,c}}{f_{-1}}\right)^2 + \left(\frac{\tau_{a,c}}{t_{-1}}\right)^2 + k\left(\frac{\sigma_{a,c}^H}{f_{-1}}\right)^2} = \beta \quad (2)$$

where $\sigma_{m,max}$ is the mean normal stress on the maximum stress amplitude plane, and f_{ref} is the reference stress, which can be calibrated using uniaxial fatigue tests with mean stress. If fatigue tests with mean stress are not available, f_{ref} can take the value of the ultimate static strength, which is same as the model by Soderberg [64].

2.3. Fatigue life model

Liu and Mahadevan [41] have extended the above fatigue limit criterion to be a fatigue life prediction model. Notice that the fatigue limit is often related to the fatigue strength at very high number of cycles (usually 10^6 – 10^7 cycles). For finite fatigue life predictions, the damage parameter should be correlated with the life (number of loading cycles to failure). Eq. (2) can be rewritten as

$$\frac{1}{\beta} \frac{1}{\left(1 - \frac{\sigma_{m,max}}{f_{ref}}\right)} \sqrt{(\sigma_{a,c})^2 + \left(\frac{f_{-1}}{t_{-1}}\right)^2 (\tau_{a,c})^2 + k(\sigma_{a,c}^H)^2} = f_{-1} \quad (3)$$

The left side of Eq. (3) can be treated as the equivalent stress amplitude. It can be used to correlate with the fatigue life using the uniaxial S–N curve. Thus the fatigue life model is expressed as:

$$\frac{1}{\beta} \frac{1}{\left(1 - \frac{\sigma_{m,max}}{f_{ref}}\right)} \sqrt{(\sigma_{a,c})^2 + \left(\frac{f_{N_f}}{t_{N_f}}\right)^2 (\tau_{a,c})^2 + k(\sigma_{a,c}^H)^2} = f_{N_f} \quad (4)$$

where N_f is the number of cycles to failure. Notice here f_{-1} and t_{-1} in Eq. (3) change to f_{N_f} and t_{N_f} respectively, which are fatigue strength coefficients at finite life N_f for uniaxial and torsional loadings. Eq. (4) has no closed form solution. In practical calculation, a trial and error method can be used to find N_f . For high cycle fatigue, f_{N_f} and t_{N_f} take initial values as f_{-1} and t_{-1} . It is found that usually a few iterations are enough to make N_f converge. Eq. (4) together with the parameters in Table 1 are used for fatigue life prediction. The quantity s in Table 1 is redefined as $s = \frac{t_{N_f}}{f_{N_f}}$.

2.4. Characteristic plane approach and critical plane approach

We named the proposed method as a characteristic approach in order to distinguish with the available critical plane-based approaches. The characteristic plane approach has some unique properties, which makes it possible to be unified for both isotropic metals and anisotropic composites. The fundamental differences of the two approaches are described as below:

1. Their physical bases are different. The critical plane approach originates from the fatigue failure mechanisms, which is usually either the maximum normal stress (strain) plane (Mode I) or the maximum shear stress (strain) plane (Mode II or III). For example, some critical plane-based approach was originally proposed based on the observations that the fatigue crack nucleation occurs at the persistent slip bands, formed in some grains (crystals) of the metals. The planes are named critical plane and the stress (or strain) components on it are used for fatigue analysis [52]. That is the physical

basis of the critical plane approach. This assumption or basis makes it difficult to apply the model to materials with microstructures different with normally used metals. The characteristic plane approach originates from the dimension reduction idea, in which the main objective is to reduce the complexity of the multiaxial fatigue problem. The resulting characteristic plane is only a material plane, on which the fatigue damage is evaluated. It may or may not have a direct relation with the fatigue crack orientation observed in the experiments. The physical difference makes the characteristic plane approach capable to the non-metals, such as composite laminates used in this study, in which the non-crystal like microstructure violates the physical basis of the critical plane approach. Also, the physical difference makes the characteristic plane approach not require failure modes analysis before application to multiaxial fatigue damage calculation, which is usually required by the critical plane-based models [14].

2. The identification procedures of the characteristic plane and the critical plane are different. Once the material failure mode is observed, the identification of the critical plane is straightforward. It only relies on stress (or strain) analysis. For different materials with the same failure mode, the critical plane orientation is fixed. It is either the maximum normal stress (or strain) plane or the maximum shear stress (or strain) plane. The characteristic plane in the proposed model is determined through minimizing the contributions of the hydrostatic strain amplitude to zero (as shown in Section 2.1). It explicitly relies both on the material properties and stress (strain) analysis. For different materials with the same failure mode, the characteristic plane could be different since it depends on both the uniaxial and pure torsional S–N curves. From this point of view, the determination of the critical plane is semi-analytical because it requires that the analyst determine the failure modes first from experimental data or assumes from experience. The characteristic plane determination is fully analytical since it only requires the quantitative data from uniaxial and torsional experiments.
3. The results and robustness of the characteristic plane approach and the critical plane approach are different. The result of the critical plane is a discrete function, which is either maximum normal strain plane or maximum shear strain plane. The result of the characteristic plane is a quantitative and continuous function. In the multiaxial fatigue experiments for metals, usually both Mode I and Mode II cracks exist. For example, under pure shear tests, the crack usually occurs along the maximum shear stress plane then propagates along the maximum principle stress plane. In that case, only visual or empirical observation is not good enough to decide which model to use. Also, if you make a decision based on a certain parameter exceeding a threshold value (e.g. Life of Mode II crack exceeds 70% of the total life), there is still a problem because you create a discontinu-

ity subjectively. The material with 69% uses the critical plane of maximum normal stress amplitude and the material with 71% uses the critical plane which is 45° off the maximum normal stress amplitude plane. Therefore, a quantitative and continuously varying model is more desirable. For the material changing failure modes with respect to loadings and environmental conditions or the material without failure mode information, it is risky to apply either of those models (i.e. based on Mode I or Mode II crack), because their error is unpredictable. From this point of view, the proposed model is more robust since it can automatically adapt to those conditions.

From the above discussion, it is clearly shown that the reason why the characteristic plane-based approach can be applied to very different materials, which is due to the proposed method does not rely on the failure mechanism or material microstructures.

3. New multiaxial fatigue model for anisotropic material

Many engineering materials exhibit mechanical anisotropy, such as wood, rolled metals, fiber reinforced composite laminates, etc. The uniaxial and torsional fatigue strengths also depend on the orientations of the axes at the critical point within the material. In the proposed multiaxial fatigue criterion (Eq. (1)), fatigue limits f_{-1} and t_{-1} become functions of the orientation θ , say, $f_{-1}(\theta)$ and $t_{-1}(\theta)$. A schematic representation for unidirectional composite laminates is shown in Fig. 1. The x -axis is along the fiber direction and the y -axis is transverse to the fiber direction. Due to the strong fiber strength and weak matrix strength, the laminate is orthotropic. Fatigue strength at the arbitrary orientation θ is different and is a function of θ .

In order to extend the fatigue model (Eq. (1)) to anisotropic materials, we need to specify a reference plane, on which the uniaxial and torsional strength of the anisotropic material can be evaluated. In the current model, the key point is to calculate the angle between the maximum normal stress amplitude plane and the characteristic plane. We define the reference plane for the anisotropic material as the plane that experiences the maximum normal stress

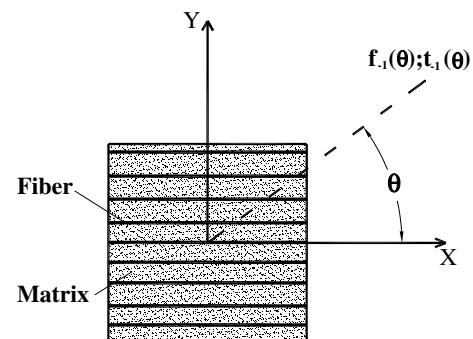


Fig. 1. Fatigue strength for unidirectional laminates.

amplitude. Thus, Eq. (1) is rewritten as a unified multiaxial fatigue criterion:

$$\sqrt{\left(\frac{\sigma_{a,z}}{f_{-1}(\theta_{\max})}\right)^2 + \left(\frac{\tau_{a,z}}{t_{-1}(\theta_{\max})}\right)^2 + k\left(\frac{\sigma_{a,z}^H}{f_{-1}(\theta_{\max})}\right)^2} = \beta \quad (5)$$

where θ_{\max} indicates the direction of maximum stress amplitude. For isotropic materials, Eq. (5) reduces to Eq. (1) since the functions $f_{-1}(\theta)$ and $t_{-1}(\theta)$ become constants. Similarly, the fatigue life model for anisotropic materials can be expressed as:

$$\frac{1}{\beta} \sqrt{(\sigma_{a,c})^2 + \left(\frac{f_{N_f}(\theta_{\max})}{t_{N_f}(\theta_{\max})}\right)^2 (\tau_{a,c})^2 + k(\sigma_{a,c}^H)^2} = f_{N_f}(\theta_{\max}) \quad (6)$$

Eq. (6) can be rewritten as:

$$\frac{1}{p_{N_f}(\theta_{\max})} \frac{1}{\beta} \sqrt{(\sigma_{a,c})^2 + \left(\frac{1}{s_{N_f}(\theta_{\max})}\right)^2 (\tau_{a,c})^2 + k(\sigma_{a,c}^H)^2} = f_{N_f}(0) \quad (7)$$

If the mean stress is also included into the model, Eq. (8) could be used.

$$\frac{1}{\left(1 - \frac{\sigma_{m,\max}}{f_{ref}}\right)} \frac{1}{p_{N_f}(\theta_{\max})} \frac{1}{\beta} \times \sqrt{(\sigma_{a,c})^2 + \left(\frac{1}{s_{N_f}(\theta_{\max})}\right)^2 (\tau_{a,c})^2 + k(\sigma_{a,c}^H)^2} = f_{N_f}(0) \quad (8)$$

where $s_{N_f}(\theta_{\max}) = \frac{t_{N_f}(\theta_{\max})}{f_{N_f}(\theta_{\max})}$ is the strength ratio of the torsional loading and the uniaxial loading along the direction of θ_{\max} . $p_{N_f}(\theta_{\max}) = \frac{f_{N_f}(\theta_{\max})}{f_{N_f}(0)}$ is the ratio of uniaxial strength along the directions of $\theta = \theta_{\max}$ and $\theta = 0$. The left side of Eq. (8) can be treated as an equivalent stress amplitude. It can be used to correlate with the fatigue life using the uniaxial S–N curve along the direction of zero degree.

The procedure for the fatigue analysis of anisotropic materials is almost identical with that of isotropic material. For any arbitrary loading history, the maximum stress amplitude plane is identified first. The uniaxial and torsional fatigue strength along this direction is also evaluated, usually from experimental data. Then the angle α and the material parameters are determined for different materials according to Table 1. Notice that, the quantity s in Table 1 is now redefined as $s = s_{N_f}(\theta_{\max}) = \frac{t_{N_f}(\theta_{\max})}{f_{N_f}(\theta_{\max})}$. Finally the equivalent stress amplitude and the fatigue life are calculated using Eq. (7) (or Eq. (8)) if mean stress is included.

For an arbitrary anisotropic material, the variation of the uniaxial and torsional fatigue strengths corresponding to the orientation of the axes is quite complex and requires extensive experimental work to quantify. However, for some special anisotropic materials, this can be simplified using one of strength theories available in the literature. In this paper, an example of orthotropic composite laminate is used for illustration.

Consider a fiber reinforced composite laminate. Several static strength theories have been proposed for orthotropic laminates, such as Tsai-Hill and Tsai-Wu theory [9]. In this study, the Tsai-Wu theory is used. For the case of plane stress, the Tsai-Wu theory is expressed as:

$$F_{11}\sigma_1^2 + F_{22}\sigma_2^2 + F_{66}\sigma_6^2 + F_1\sigma_1 + F_2\sigma_2 + 2F_{12}\sigma_1\sigma_2 = 1 \quad (9)$$

where σ_1 and σ_2 are the stresses along the fiber direction and transverse to the fiber direction, respectively, and σ_6 is the in-plane shear stress. F_{11} , F_{22} , F_{66} , F_{12} , F_1 , and F_2 are strength parameters and can be calibrated using experiments.

$$\begin{cases} F_{11} = \frac{1}{s_L^+ s_L^-}, & F_1 = \frac{1}{s_L^+} - \frac{1}{s_L^-}, & F_{22} = \frac{1}{s_T^+ s_T^-}, & F_2 = \frac{1}{s_T^+} - \frac{1}{s_T^-} \\ F_{66} = \frac{1}{s_{LT}^2}, & F_{12} = -\frac{(F_{11}F_{22})^2}{2} \end{cases} \quad (10)$$

where $s_L^{(\pm)}$, $s_T^{(\pm)}$ are the strengths along the fiber direction and transverse to the fiber direction, respectively. The plus symbol indicates tension strength and the minus symbol indicates compression strength. s_{LT} is the in-plane shear strength. For the fatigue problem, the stress terms in Eq. (9) refer to the stress amplitudes along different directions. If the strengths are defined using stress amplitude values, the plus and minus symbols in the above strength notation disappear since the stress amplitude is always positively defined. Thus, Eqs. (9) and (10) are rewritten for the fatigue problem as:

$$F_{11}\sigma_1^2 + F_{22}\sigma_2^2 + F_{66}\sigma_6^2 + 2F_{12}\sigma_1\sigma_2 = 1 \quad (11)$$

$$\begin{cases} F_{11} = \frac{1}{s_L^2}, & F_{22} = \frac{1}{s_T^2}, & F_{66} = \frac{1}{s_{LT}^2}, & F_{12} = -\frac{(F_{11}F_{22})^2}{2} \end{cases} \quad (12)$$

Using the Tsai-Wu strength theory, the uniaxial strength and shear strength along an arbitrary direction θ can be easily obtained as

Table 2
Experimental data for isotropic metals

Material	References	Failure mechanism
SAE-1045 steel	Kurath et al. [36]	N/A
5% Chrome work roll steel	Kim et al. [34]	Tensile
SM45C	Lee [39]	N/A
7010 Aluminum alloy	Chaudonneret [6]	N/A
Waspaloy	Jayaraman and Ditmars [23]	Shear
	Learch et al. [38]	
Hastelloy-X	Jordan [25]	23 °C: shear; 649 °C: tensile
Hayness 188	Bonacuse et al. [2] Kalluri et al. [30]	N/A
Ti–6Al–4V alloy	Kallmeyer et al. [29]	Not performed
AISI Type 304 stainless steel	Socie [62]	Tensile
Z12CNDV12-2 steel	Chaudonneret [6]	N/A

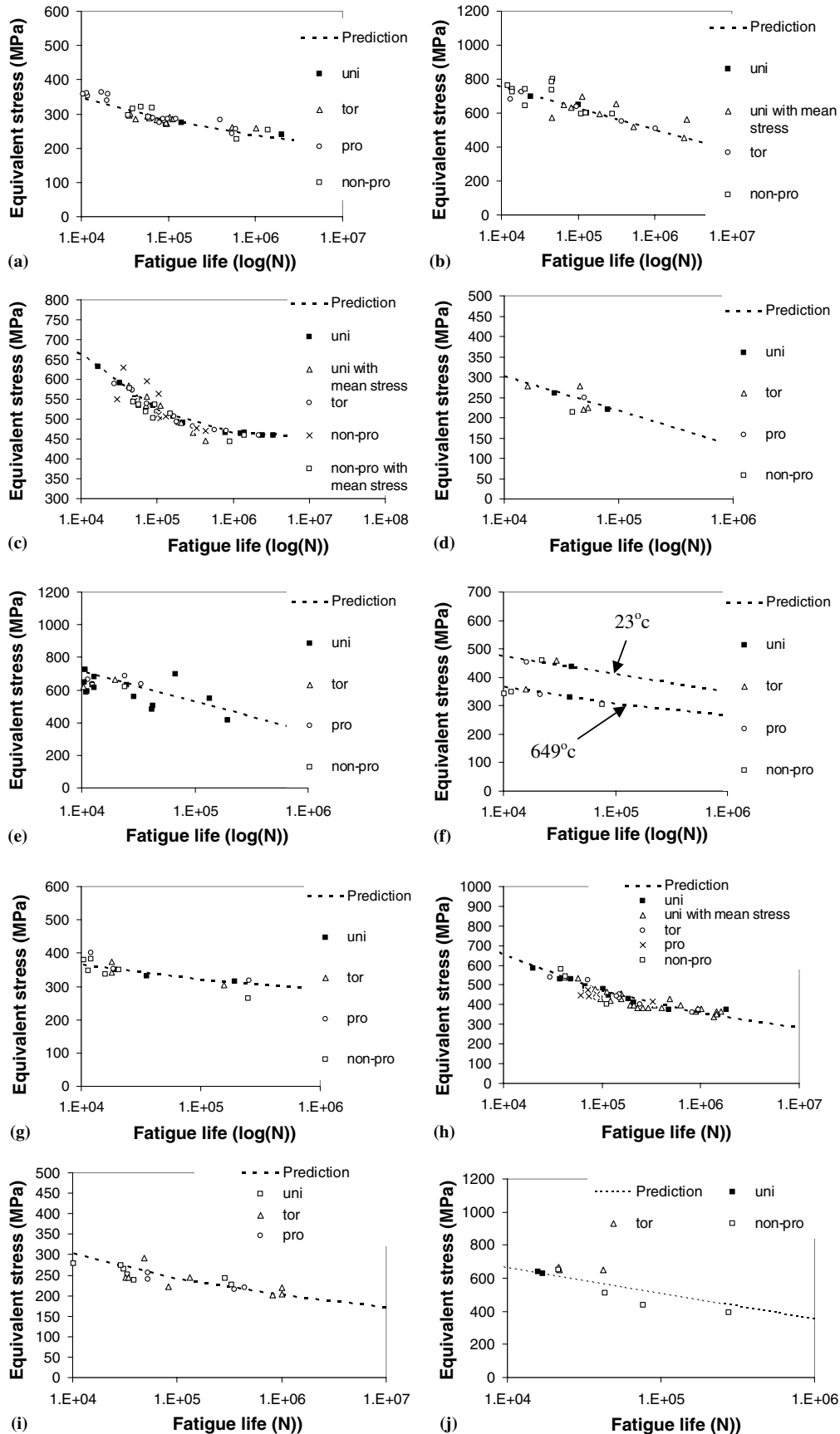


Fig. 2. Comparisons of predicted and experimental fatigue lives: (a) SAE-1045 steel. (b) 5% Chrome work roll steel. (c) SM45C steel. (d) 7010 Aluminum alloy. (e) Waspaloy. (f) Hastelloy-X. (g) Haynes 188. (h) Ti-6Al-4V alloy. (i) AISI Type 304 stainless steel. (j) Z12CNDV12-2 steel.

$$\begin{cases} f(\theta) = 1/\sqrt{F_{11}\cos^4\theta + F_{22}\sin^4\theta + (F_{66} + 2F_{12})\sin^2\theta\cos^2\theta} \\ t(\theta) = 1/\sqrt{(F_{11} + F_{12} - 8F_{12})\sin^2\theta\cos^2\theta + F_{66}(\cos^2\theta - \sin^2\theta)^2} \end{cases} \quad (13)$$

For the fatigue life model, the fatigue strength parameters are also functions of the fatigue life (N_f), which can be evaluated from the experimental S–N curves. Eq. (13) is rewritten as:

$$\begin{cases} f_{N_f}(\theta) = 1/\sqrt{F_{11,N_f}\cos^4\theta + F_{22,N_f}\sin^4\theta + (F_{66,N_f} + 2F_{12,N_f})\sin^2\theta\cos^2\theta} \\ t_{N_f}(\theta) = 1/\sqrt{(F_{11,N_f} + F_{12,N_f} - 8F_{12,N_f})\sin^2\theta\cos^2\theta + F_{66,N_f}(\cos^2\theta - \sin^2\theta)^2} \end{cases} \quad (14)$$

Substituting Eq. (14) into Eq. (8), we can solve for the fatigue life (N_f). Similar to isotropic materials, Eq. (8) usually has no closed form solution. In practical calculation, a trial and error method can be used to find N_f . For an orthotropic composite laminate, the experimental S–N curves along the fiber direction, transverse to the fiber direction, and in-plane shear stress are required in the proposed model. Then the fatigue life under arbitrary multiaxial loading can be predicted.

The fatigue model for the isotropic material in Section 2 is consistent with the fatigue model for the anisotropic material derived in Section 3. If $F_{11} = F_{22} = \frac{1}{3}F_{66}$, the fatigue model for the orthotropic material is identical with the fatigue model for the isotropic material with $s = 1/\sqrt{3}$, in which the Tsai-Wu criterion reduces to be the Von-Mises criterion.

4. Validation of the proposed fatigue model

In this section, the proposed multiaxial fatigue life prediction model is validated using experimental observations found in the literature. Three categories of data are explored: metals for isotropic material, unidirectional composite laminates for orthotropic material and multidirectional composite laminates for anisotropic material.

4.1. Validation for isotropic material

Ten sets of fatigue experimental data are employed in this section, and are listed in Table 2. The collected materials cover several different industries, such as construction engineering, automotive engineering, and aerospace engineering and range from brittle to ductile. Different failure mechanisms are also listed in Table 2 to show the applicability of the proposed characteristic plane-based method.

The S–N curve approach is commonly used for the HCF problem and the e–N curve approach is commonly used for the LCF problem. The proposed characteristic plane based approach has been validated for both the HCF problem using S–N curves [41] and the LCF problem using e–N curves [43]. Since the experimental data for composite laminates is usually stress-controlled and belongs to the HCF

fatigue problem, the current study uses the S–N curve version of the characteristic plane approach. In the revised manuscript, we only keep the metal fatigue data with the fatigue life ranging from 10^4 to 10^7 cycles, which belongs in the intermediate to high cycle fatigue. For the LCF problem using the characteristic plane-based approach, the reader is referred to our previous e–N curve paper [42].

The predicted fatigue lives and the experimental lives are plotted together in Fig. 2. In Fig. 2, the x -axis is the fatigue

life in log scale and the y -axis is the equivalent stress amplitude which is calculated from Eq. (4). The dashed lines are the prediction results and the points are the experimental observations. In the legends, “uni” represents uniaxial loading, “tor” represents pure torsional loading, “pro” represents proportional multiaxial loading and “non-pro” represents non-proportional multiaxial loading. For data sets where mean stress data is available, mean stress effect is also included in the results.

In the proposed method for isotropic materials, only the uniaxial and pure torsional fatigue S–N curves are required to calibrate the material parameters (fatigue strength coefficients at finite life N_f for uniaxial and torsional loadings, f_{N_f} and t_{N_f} , respectively). All other proportional or non-proportional multiaxial fatigue data are “predictions” to show the performance of the proposed method.

As shown in Fig. 2, the predicted results agree very well with the experimental results despite different amounts of scatter for different materials. For different materials and loading conditions, the proposed model correlates the experimental observations together using the uniaxial fatigue S–N curve.

4.2. Validation for unidirectional composite laminates

Eight sets of fatigue experimental data for unidirectional composite laminate under off-axis loading are employed in this section, and are listed in Table 3.

Table 3
Experimental data for unidirectional composite laminates

Material	References
E-glass/polyester	Philippidis and Vassilopoulos [54]
E-glass fibre/epoxy-1	Kadi and Ellyin [26]
T800H/epoxy	Kawai et al. [31]
T800H/polyimide	Kawai et al. [31]
AS4/PEEK	Kawai et al. [31]
GLARE 2 (fibre–metal laminates)	Kawai et al. [31]
T800H/2500 carbon/epoxy	Kawai and Suda [33]
E-glass fibre/epoxy-2	Hashin and Rotem [22]
	Reported by Petermann and Plumtreeb [53]

In the proposed fatigue life model for orthotropic materials, experimental S–N curves for the fiber direction, transverse to the fiber direction, and pure in-plane shear stress are required. However, most of the fatigue experimental data do not include the pure shear test results. It is possibly due to the difficulty of applying the pure shear loading to the composite laminate. The S–N curve under pure shear loading is calibrated using one additional off-axis fatigue

test data set and then used for fatigue life prediction for the other off-axis fatigue loadings. For example, the T800H/epoxy fatigue data reported Kawai and Suda [33] contains the S–N curves along the fiber direction (0° laminates) and transverse to the fiber direction (90° laminates). Pure in-plane shear fatigue tests were not performed. The fatigue data for 45° laminates is used to calibrate the pure in-plane shear S–N curve by a trial and error method. After

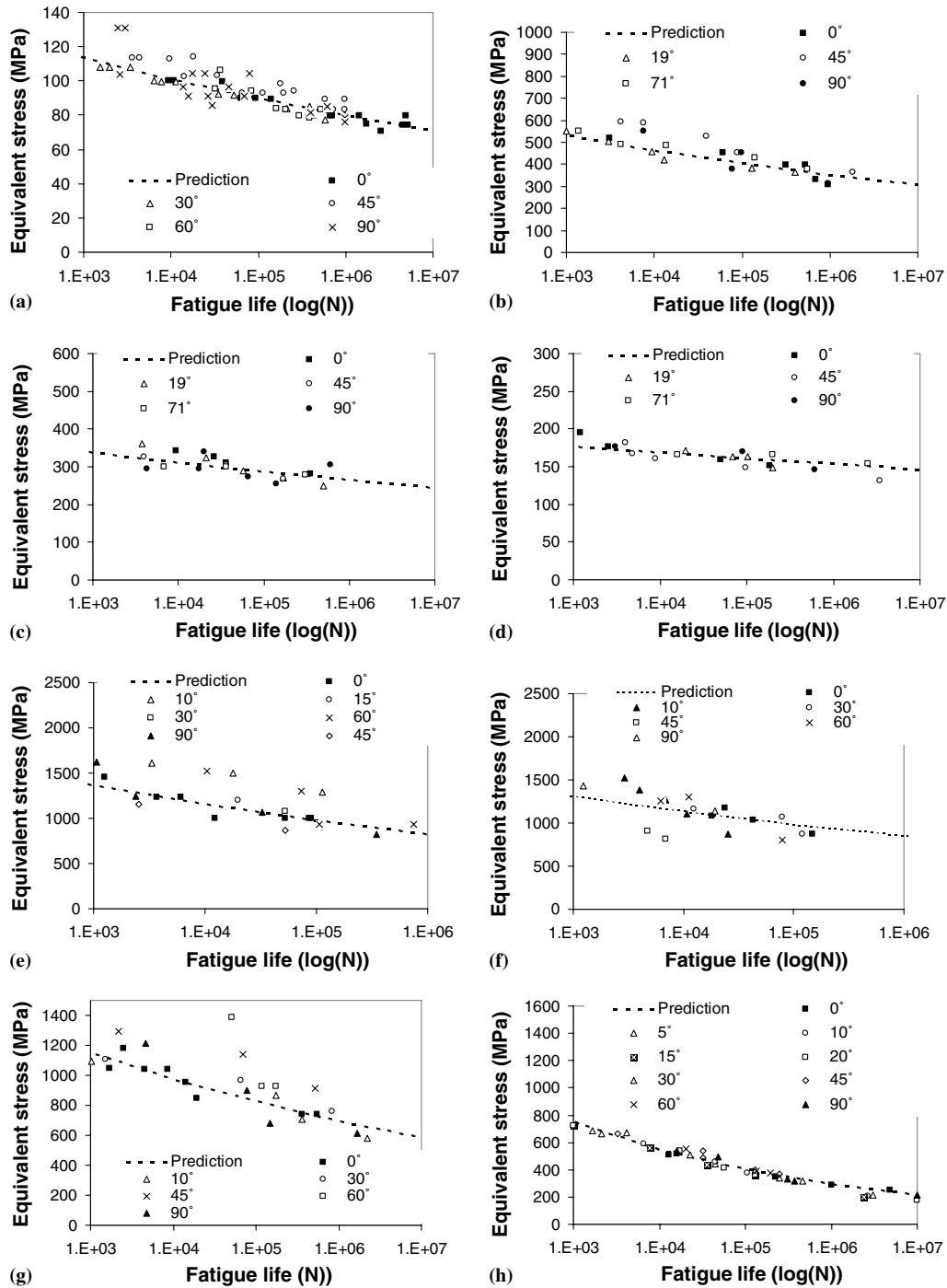


Fig. 3. Comparisons of predicted and experimental fatigue lives for unidirectional composite laminates: (a) E-glass/polyester. (b) E-glass fibre/epoxy-1 with $R = -1$. (c) E-glass fibre/epoxy-1 with $R = 0$. (d) E-glass fibre/epoxy-1 with $R = 0.5$. (e) T800H/epoxy. (f) T800H/polyimide. (g) AS4/PEEK. (h) GLARE 2. (i) T800H/2500 carbon/epoxy with $R = 0.5$. (j) T800H/2500 carbon/epoxy with $R = 0.1$. (k) T800H/2500 carbon/epoxy with $R = -0.3$. (l) E-glass fibre/epoxy-2.

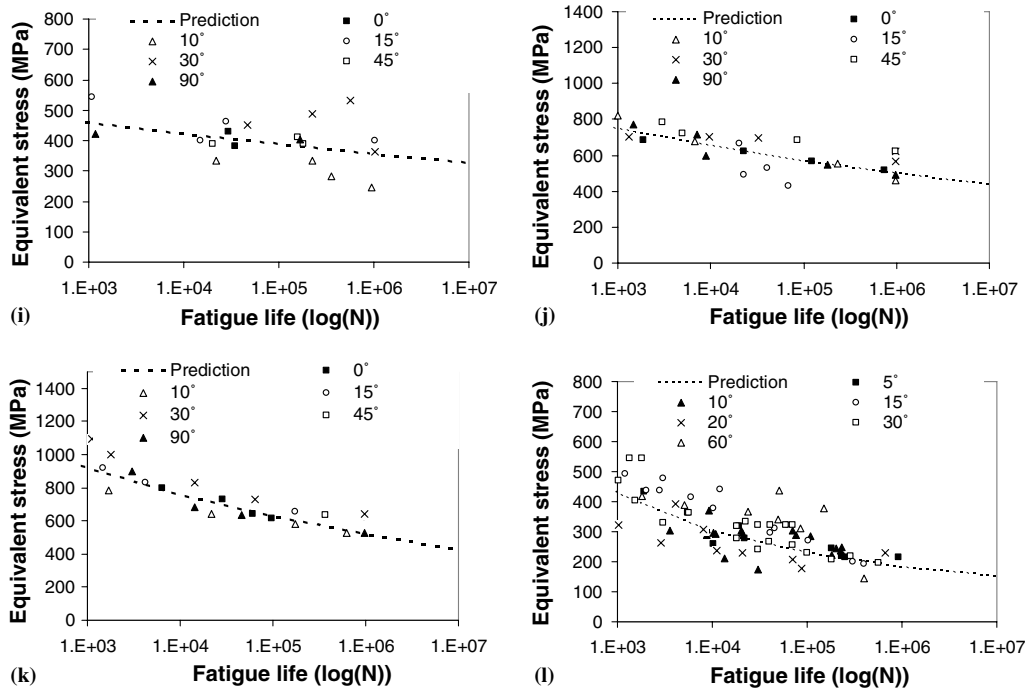


Fig. 3 (continued)

obtaining the three S–N curves required in the proposed method, the fatigue life of composite laminates with arbitrary orientations (10°, 15°, 30° and 60° in this case) can be predicted.

The predicted fatigue lives and the experimental lives are plotted together in Fig. 3. In Fig. 3, the x-axis is the fatigue life in log scale and the y-axis is the equivalent stress amplitude which is calculated from Eq. (8). The dashed lines are the prediction results and the points are the experimental observations. The angles of the off-axis loading are shown in the legends. Only some of the references in Table 3, namely, Kadi and Ellyin, Kawai and Suda [26,33] include the mean stress effect on the fatigue life. Figs. 3(b)–(d) include this stress ratio, which is defined as the minimum stress divided by the maximum stress.

As shown in Fig. 3, the predicted results agree reasonably well with the experimental results despite different amounts of scatter for different materials. Generally speak-

ing, the scatter for composite laminates is larger than that for metals. The worst case is for E-glass fibre/epoxy-2 (Fig. 3(l)). In the original data, very large scatter was observed. A probabilistic approach may be more appropriate to describe the fatigue behavior of composite materials.

4.3. Validation for multidirectional composite laminates

Composite structures are more likely to be in the form of multidirectional laminates consisting of multiple laminates or plies, which may have different ply orientations and stacking sequences. Due to the arbitrary combinations of the plies, the macro-mechanical properties of the multidirectional composite laminates are anisotropic. The fatigue analysis is more complicated than that for unidirectional composite laminates and requires extensive experimental work to quantify the effect of anisotropy. However, multidirectional composite laminates are built

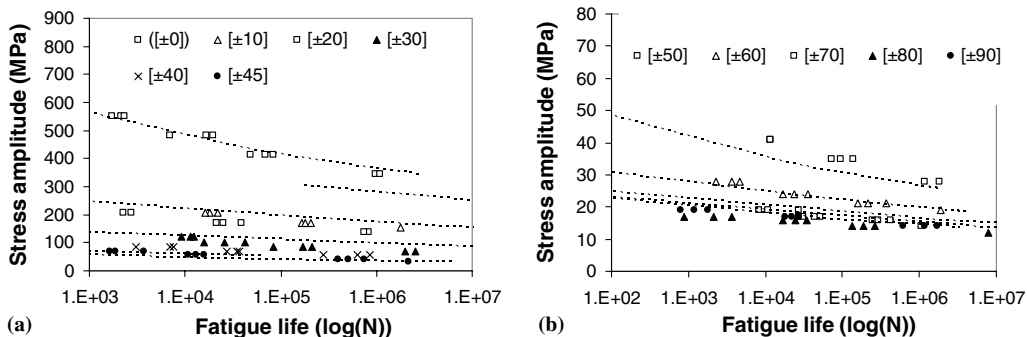


Fig. 4. Comparisons of predicted and experimental fatigue lives for D155 with $R = 0.1$.

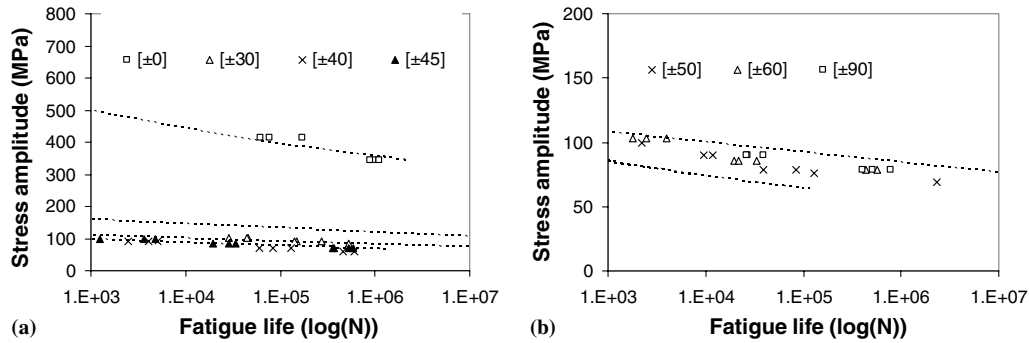


Fig. 5. Comparisons of predicted and experimental fatigue lives for D155 with $R = 10$.

up with many orthotropic plies. For this type of material, the authors [42] developed a two-stage methodology for the fatigue analysis. First, divide the total loading history into several blocks. In each block, check the failure of each ply using the fatigue model. If no failure occurs, accumulate the fatigue damage for each ply caused in this block and progress to the next step. If failure occurs, assume that the ply strength and stiffness decrease to zero. Then update the global stiffness matrix and progress to the next step. The computation is continued till the entire laminate fails. This section uses this methodology. In each ply, the fatigue model derived in Section 3 is used to check the failure.

Fatigue test data of glass–fiber-based multidirectional composite laminates [46] are used to validate the proposed fatigue model. The material chosen, D155, is a balanced laminate which consists of pairs of layers with identical thicknesses and elastic properties but with $+\theta$ and $-\theta$ orientations. Again, the fatigue S–N curve for pure shear test is not available and the balanced laminate ($[\pm 45]_3$) is used to calibrate the in-plane shear S–N curve.

The prediction results and the experimental observations are plotted in Figs. 4 and 5. The x -axis is the fatigue life and the y -axis is the applied stress amplitude. The dashed lines are the prediction results and the points are experimental results. From Figs. 4 and 5, the agreement is seen to be generally very good, with a few exceptions. In all cases, the predictions capture the major trends in the experimental observations.

5. Conclusions

A unified multiaxial fatigue life prediction model is proposed in this paper for both isotropic and anisotropic materials. The current fatigue model is based on the characteristic plane approach. Most of the existing critical plane-based models can only be applied to certain types of failure modes, i.e. shear dominated failure or tensile dominated failure. Their applicability generally depends on the material's properties and loading conditions. In the proposed model, the characteristic plane changes corresponding to different material failure modes, thus making the proposed model have almost no applicability limitation with respect to different

metals. The characteristic plane is theoretically determined by minimizing the damage introduced by the hydrostatic stress amplitude. The mean normal stress effect is also included in the current model through a correction factor. The proposed method does not consider the mean shear stress effect since no mean shear stress exists in the collected data. Its effect on the multiaxial fatigue needs extensive experimental and theoretical work in the future.

A wide range of fatigue data, which covers both brittle and ductile metals, as well as unidirectional and multidirectional composite laminates, are used to validate the proposed methodology. Generally, the predictions based on the proposed model agree well with the experimental observations.

The fatigue data collected in this study for composite laminates are under off-axis loading, which causes proportional multiaxial stress within the material. The test data for composite laminates under non-proportional loading are seldom found in the literature. The proposed model has been validated under non-proportional loadings for isotropic metals. Further experimental data are needed to validate the proposed model under non-proportional loading for anisotropic materials.

References

- [1] ASME. Cases of ASME boiler and pressure vessel code. New York: American Society of Mechanical Engineers; 1979.
- [2] Bonacuse PJ, Kalluri S. Elevated temperature axial and torsional fatigue behavior of Haynes 188, NASA Center for AeroSpace Information (CASI) NASA-TM-105396; E-6788; NAS 1.15:105396; AVSCOM-TR-91-C-045, 19920601, 1992.
- [3] Brown MW, Miller KJ. Two decades of progress in the assessment of multiaxial low-cycle fatigue life. In: Amzallag C, Leis B, Rabbe P, editors. Low-cycle fatigue and life prediction. ASTM STP 770. Philadelphia: ASTM; 1982. p. 482–99.
- [4] Brown MW, Miller KJ. A theory for fatigue failure under multiaxial stress–strain conditions. Proc Inst Mech Eng 1973;187:745–55.
- [5] Carpinteri A, Spagnoli A. Multiaxial high-cycle fatigue criterion for hard metals. Int J Fatigue 2001;23:135–45.
- [6] Chaudonneret M. A simple and efficient multiaxial fatigue damage model for engineering applications of macro-crack initiation. J Eng Mater Technol 1993;115:373–9.
- [7] Chu CC, Conle FA, Bonnen JJ. Multiaxial stress–strain modeling and fatigue life prediction of SAE axle shafts. In: McDowell DL, Ellis R,

- editors. *Advances in multiaxial fatigue*. ASTM STP 1191. Philadelphia: ASTM; 1993. p. 37–54.
- [8] Crossland B. Effect of large hydrostatic pressures on the torsional fatigue strength of an alloy steel. In: *Proceedings of the international conference on fatigue of metals*. London: Institution of Mechanical Engineers; 1956. p. 138–49.
- [9] Daniel IM, Ishai O. *Engineering mechanics of composite materials*. New York: Oxford University Press; 1994.
- [10] Davoli P, Bernasconi A, Filippini M, Foletti S, Papadopoulos IV. Independence of the torsional fatigue limit upon a mean shear stress. *Int J Fatigue* 2003;25(6):471–80.
- [11] Degrieck J, Van Paepegem W. Fatigue damage modelling of fibre-reinforced composite materials: review. *Appl Mech Rev* 2001;54(4):279–300.
- [12] Diao X, Lessard L, Shokrieh M. Statistical model for multiaxial fatigue behavior of unidirectional plies. *Compos Sci Technol* 1999;59:2025–35.
- [13] Farahani AV. A new energy critical plane parameter for fatigue life assessment of various metallic materials subjected to in-phase and out-of-phase multiaxial fatigue loading conditions. *Int J Fatigue* 2000;22:295–305.
- [14] Fatemi A, Socie DF. A critical plane approach to multiaxial fatigue damage including out of phase loading. *Fatigue Fract Eng Mater Struct* 1988;11:149–65.
- [15] Findley WN. A theory for the effect of mean stress on fatigue of metals under combined torsion and axial load or bending. *J Eng Ind, Trans ASME* 1959;81:301–6.
- [16] Fround MS. In: Miller KJ, Brown MW, editors. *Multiaxial fatigue*. ASTM STP 853. Philadelphia: American Society for Testing and Materials; 1985. p. 381–95.
- [17] Garud YS. Multiaxial fatigue: a survey of the state-of-the-art. *J Test Evaluation* 1981;9:165–78.
- [18] Gerber H. Bestimmung der zulässigen Spannungen in Eisen-konstruktionen. *Zeitschrift des Bayerischen Architekten und ingenieur-Vereins* 1874;6:101–10.
- [19] Glinka G, Plumtree A, Shen G. A multiaxial fatigue strain energy parameter related to the critical plane. *Fatigue Fract Eng Mater Struct* 1995;18:37–46.
- [20] Goodman J. *Mechanics applied to engineering*. London: Longmans Green; 1899.
- [21] Gough HJ, Pollard HV, Clenshaw WJ. Some experiments on the resistance of metals to fatigue under combined stresses, Aeronautical Research Council Reports, R and M 2522, London: HMSO; 1951.
- [22] Hasin Z, Rotem A. A fatigue criterion for fiber reinforced composite material. *J Compos Mater* 1973;7:448–64.
- [23] Jayaraman N, Ditmars MM. Torsional and biaxial (tension–torsion) fatigue damage mechanisms in Waspaloy at room temperature. *Int. J. Fatigue* 1989;11:309–18.
- [24] Jen MHR, Lee CH. Strength and life in the thermalplastic composite laminates under static and fatigue loads. *Int J Fatigue* 1998;20:605–15.
- [25] Jordan EH. Elevated temperature biaxial fatigue. NASA Center for Aerospace Information (CASI), NASA-CR-175009; NAS 1.26:175009, 19851001, 1985.
- [26] Kadi El, Ellyin HF. Effect of stress ratio on the fatigue of unidirectional glass fibre/epoxy composite laminae. *Composites* 1994;25:917–24.
- [27] Kandil FA, Brown MW, Miller KJ. Biaxial low cycle fatigue fracture of 316 stainless steel at elevated temperatures, vol. 280. London: The Metal Society; 1982. p. 203–10.
- [28] Kakuno H, Kawada Y. A new criterion of fatigue strength of a round bar subjected to combined static and repeated bending and torsion. *Fatigue Eng Mater Struct* 1979;2(2):229–36.
- [29] Kallmeyer AR, Ahmo K, Kurath P. Evaluation of multiaxial fatigue life prediction methodologies for Ti–6Al–4V. *J Eng Mater Technol Trans ASME* 2002;124:229–37.
- [30] Kalluri S, Bonacuse PJ. In-phase and out-of-phase axial-torsional fatigue behavior of Haynes 188 at 760 C, NASA Center for Aerospace Information (CASI), NASA-TM-105765; E-7182; NAS 1.15:105765; AVSCOM-TR-91-C-046; Symposium on multiaxial fatigue, San Diego, CA, United States, 19911001, 1991.
- [31] Kawai M, Hachinohe A, Takumida K, Kawase Y. Off-axis fatigue behaviour and its damage mechanics modelling for unidirectional fibre–metal hybrid composite: GLARE 2. *Composites: Part A* 2001;32:13–23.
- [32] Kawai M. A phenomenological model for off-axis fatigue behavior of unidirectional polymer matrix composites under different stress ratios. *Composites: Part A* 2004;35:955–63.
- [33] Kawai M, Suda H. Effects of non-negative mean stress on the off-axis fatigue behavior of unidirectional carbon/epoxy composites at room temperature. *J Compos Mater* 2004;38:833–54.
- [34] Kim KS, Nam KM, Kwak GJ, Hwang SM. A fatigue life model for 5% chrome work roll steel under multiaxial loading. *Int J Fatigue* 2004;26(7):683–9.
- [35] Kujawski D, Ellyin F. A unified approach to mean stress effect on fatigue threshold conditions. *Int J Fatigue* 1995;17:101–6.
- [36] Kurath P, Downing SD, Galliard D. Summary of non-hardened notched shaft round robin program. In: Leese GE, Socie DF, editors. *Multiaxial fatigue: analysis and experiments*, SAE, AE-14. Warrendale: SAE; 1989. p. 12–32.
- [37] Langer BF. Design of pressure vessels involving fatigue. In: Nichols RW, editor. *Pressure vessel engineering*. Amsterdam: Elsevier; 1979. p. 59–100.
- [38] Learch BA, Jayaraman A, Antolovice SD. A study of fatigue damage mechanism in Waspaloy from 25 to 800 °C. *Mater Sci Eng* 1984;66:151–66.
- [39] Lee SB. Out-of-phase bending and torsion fatigue of steels. In: Brown MW, Miller KJ, editors. *Biaxial and multiaxial fatigue*, EGF3. London: Mechanical Engineering Publications; 1989. p. 612–34.
- [40] Lin H, Nayeb-Hashemi H, Pelloux RM. A multiaxial fatigue damage model for orthotropic materials under proportional loading. *Fatigue Fract Eng Mater Struct* 1993;16:723–42.
- [41] Liu Y, Mahadevan S. Multiaxial high-cycle fatigue criterion and life prediction for metals. *Int J Fatigue* 2005;7(7):790–800.
- [42] Liu Y, Mahadevan S. Probabilistic fatigue life prediction of multi-directional composite laminates. *Compos Struct* 2005;69:11–9.
- [43] Liu Y, Mahadevan S. Stain based multiaxial fatigue damage modeling. *Fatigue Fract Eng Mater Struct* 2005;28:1177–89.
- [44] Lohr RD, Ellison EG. A simple theory for low cycle multiaxial fatigue. *Fatigue Fract Eng Mater Struct* 1980;3:1–17.
- [45] Macha E, Sonsino CM. Energy criteria of multiaxial fatigue failure. *Fatigue Fract Eng Mater Struct* 1999;22:1053–70.
- [46] Mandell JF, Samborsky DD. DOE/MSU composite materials fatigue database: test methods, materials, and analysis. Albuquerque, NM: Sandia National Laboratories; 2003.
- [47] Mataka T. An explanation on fatigue limit under combined stress. *Bull JSME* 1977;20:257–63.
- [48] McDiarmid DL. Fatigue under out-of-phase bending and torsion. *Fatigue Eng Mater Struct* 1987;9(6):457–75.
- [49] Morrow JD. *Fatigue design handbook – advances in engineering*, vol. 4. Warrendale, PA: Society of Automotive Engineers; 1968. Section 3.2, p. 21–9.
- [50] Pan WF, Hung CY, Chen LL. Fatigue life estimation under multiaxial loadings. *Int J Fatigue* 1999;21:3–10.
- [51] Papadopoulos IV, Davoli P, Gorla C, Filippini M, Bernasconi A. A comparative study of multiaxial high-cycle fatigue criteria for metals. *Int J Fatigue* 1997;19:219–35.
- [52] Papadopoulos IV. Long life fatigue under multiaxial loading. *Int J Fatigue* 2001;23:839–49.
- [53] Petermann J, Plumtree A. A unified fatigue failure criterion for unidirectional laminates. *Composites: Part A* 2001;32:107–18.
- [54] Philippidis TP, Vassilopoulos RP. Fatigue strength prediction under multiaxial stress. *J Compos Mater* 1999;33:1578–99.
- [55] Reifsnider KL, Gao Z. A micromechanics model for composite under fatigue loading. *Int J Fatigue* 1991;13:149–56.
- [56] Shokrieh M, Lessard L. Mutiaxial fatigue behavior of unidirectional plies based on uniaxial fatigue experiments-I Modelling. *Int J Fatigue* 1997;19:201–7.

- [57] Sines G. Behaviour of metals under complex stresses. In: Sines G, Waisman JL, editors. *Metal fatigue*. New York: McGraw-Hill; 1959. p. 145–69.
- [58] Sines G. The prediction of fatigue fracture under combined stresses at stress concentrations. *Bull Jpn Soc Mech Eng* 1961;4(15): 443–53.
- [60] Smith KN, Watson P, Topper TH. A stress–strain function for the fatigue of metals. *J Mater* 1970;5:767–78.
- [61] Socie D, Waill LA, Dittmer DF. Biaxial fatigue of inconel 718 including mean stress effects. In: Miller KJ, Brown MW, editors. *Multiaxial fatigue*. ASTM STP 853. Philadelphia: ASTM; 1985. p. 7–36.
- [62] Socie D. Multiaxial fatigue damage models. *J Eng Mater Technol, Trans ASME* 1987;109:293–8.
- [63] Socie D, Marquis G, editors. *Multiaxial fatigue*. Society of Automotive Engineers; 2000.
- [64] Soderberg CR. Factor safety and working stress. *Trans ASME* 1939;52:13–28.
- [65] Wang YY, Yao WX. Evaluation and comparison of several multi-axial fatigue criteria. *Int J Fatigue* 2004;26:17–25.
- [66] Wu L. Thermal and mechanical fatigue analysis of CFRP laminates. *Compos Struct* 1993;25:339–44.
- [67] You BR, Lee SB. A critical review on multiaxial fatigue assessments of metals. *Int J Fatigue* 1996;18:235–44.